

BRAIN TUMOUR SEGMENTATION AND GRADE CLASSIFICATION USING MODIFIED VGG19 WITH SUPPORT VECTOR MACHINE

SYEDSAFI. S¹*, KARTHEEBAN. K²

¹Assistant Professor, Department of Computer Applications,
Kalasalingam Academy of Research and Education (Deemed to be University),
Krishnankoil – 626 126, Tamil Nadu, India.

²Associate Professor, Department of Computer Science and Engineering,
Kalasalingam Academy of Research and Education (Deemed to be University),
Krishnankoil – 626 126, Tamil Nadu, India.

E-mail: ¹syedsafi.safi@gmail.com, ²k.kartheeban@klu.ac.in

ABSTRACT

A brain tumour is an abnormal cell growth that occurs either inside or outside the brain. Brain tumours are among the worst and most dangerous diseases in medicine. Convolutional neural networks produce the greatest results for tumour segmentation these days. BraTS2020 and real-time hospital images were employed in this method. Pre-processing, segmentation, and post-processing are the three phases of this methodology. During the pre-processing phase, Digital imaging & communications in medicine (DICOM) images converted to Neuroimaging informatics technology initiative (NIFTI), the images are resized, noise is removed, skulls removed process are done. During the segmentation phase, the Local binary pattern (LBP) features are identified and the modified VGG19 (M-VGG19) is employed to segment the tumour. The suggested approach obtained Dice similarity coefficient (DSC) values of 0.9415, 0.8898, 0.8862, and Hausdorff distance - 95th percentile (HD95) values of 5.65, 11.11, and 11.88 for whole tumour (WT), tumour core (TC), and enhanced tumour (ET) respectively, during the segmentation process. The usage of Graphics processing unit (GPU) reduced the training and testing computation time for segmentation and reached the speedup folds up to 3× compared with CPU. Tumour volumes are computed at the post-processing phase. Subsequently, this technique classified tumours into High-grade glioma (HGG) and Low-grade glioma (LGG) using Support vector machine (SVM). The BraTS dataset was trained using real-time hospital pictures, and this method got 85.71 classification accuracy.

Keywords: *MRI images, Image resize, Tumour segmentation, Feature extraction, VGG19, SVM, 3D volume, Classification*

1. INTRODUCTION

A brain tumour is an abnormal growth of cells in the brain. In the recent days there are more than 100 types of brain tumours are affecting the people [1]. The brain tumour has some common symptoms like severe headaches, seizures, nausea and vomiting, vision problems, balance issues, personality changes, weakness or numbness and difficulty in speaking or understanding. Brain tumours can be of two kinds. While secondary brain tumours start outside the brain and spread to other regions of the body, primary brain tumours form directly in the brain tissue. The brain tumour cells also have two types benign and malignant.

Benign is a non-cancer cells but malignant is a cancer cells [2].

In the malignant type tumour Glioma is a deadly type tumour and most of the adults and children are affected by this tumour. The World health organization (WHO) classified the tumours into four grades. The first two grades are (Grade I and II) come under low grade glioma (LGG) and next two grades are (Grade III and IV) come under high grade glioma (HGG) [3]. Many medical imaging methods are employed to examine the human body like: X-ray it uses the high electromagnetic waves to produce the human body internal structures. CT-scan uses X-rays to gives details about cross-sectional images of the body and Magnetic resonance imaging (MRI) uses

strong magnetic field and radio waves to create detailed images of organs and tissues [4].

When compare all the imaging techniques the MRI gives more details about the human brain because it clearly differentiates between various brain tissues, making it easier to identify abnormal growths like tumours. The MRI has different types like T1W, T2W, T1C, FLAIR. T1-Weighted (T1W) provides excellent anatomical detail and are often used with contrast agents to highlight tumours. T2-Weighted (T2W) images sensitive to water content, these images can help identify edema (swelling) around the tumour. Fluid-Attenuated Inversion Recovery (FLAIR) images suppress the signal from normal brain tissue, making tumours and lesions more visible. T1-Enhanced contrast (T1C) images involve injecting a contrast agent to improve tumour visibility and assess blood flow. The MRI multimodal images are given in Figure.1 [5].

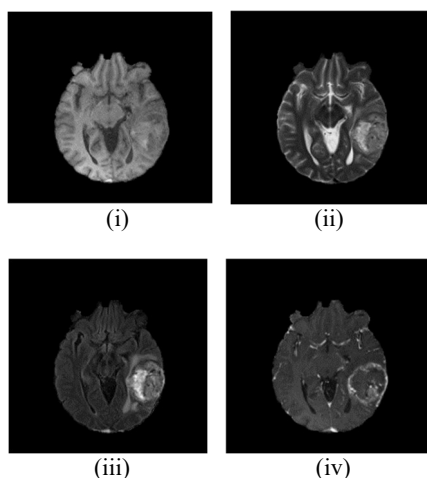


Figure 1: BRATS2020 MRI – Multimodal images
(i) T1W, (ii) T2W, (iii) TIC and (iv) FLAIR

Brain tumour segmentation is the important process to exactly identify the tumour affected cells and normal cells from the MRI images. It is very helpful to the doctors for the accurate diagnosis, tumour growth monitoring and surgical process. It segments the following sub regions from the MRI images: Whole Tumour (WT), Tumour Core (TC) and Enhanced Tumour (ET). The WT represents the overall affected areas of tumour, the TC represents the exact part of the tumour, and the ET represents the active and growing part of the tumour [6]. This type of segmentation has some common challenges: low quality images with noise, tumour boundaries are hard to find, high dimensional data, complex

tumour shapes. The tumour subregions are given in Figure.2.

The manual segmentation from the MRI multimodal images is not an easy task because it takes more time and also it did not produce accurate results. The above challenges are also affecting the manual segmentation so, this is the major reason brain tumour segmentation need automatic segmentation methods. In the recent days, Deep learning techniques are mostly used for brain tumour segmentation and, it gives a successful result [7]. The major reason for the uses of deep learning technique is: It automatically learns the complex pattern from the MRI images, it easily handles the multimodal images, it collects all the features and extract the correct patterns, it produces an accurate result and it is also used for future treatment planning.

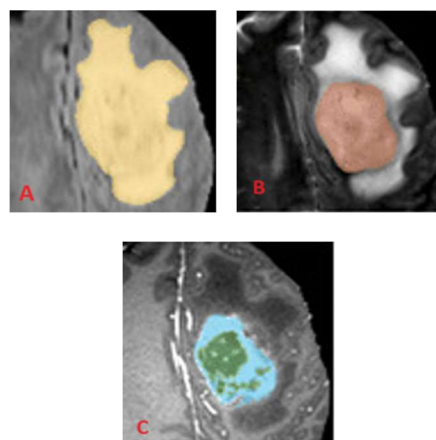


Figure 2: (A) Whole tumour (B) Tumour core and (C) Enhanced tumour

The major contribution of this manuscript is it has three phases: pre-processing, segmentation, post-processing. In the pre-processing phase: The DICOM images are convert into NIFTI, Skull removal, Noise removal and resize the images. In the Segmentation phase: extract the LBP features from the MRI images and M-VGG19 is used for tumour subregion segmentation. In the post-processing phase: The segmentation 3D parts of the WT, TC and ET are compared with the ground truth images for find the segmentation accuracy. This method also used the GPU to reduce the computation time. The proposed method processing time efficiency is calculated by speed up folds (\times). Then, Find the 3D volume of the WT and classify the tumour grades into HGG and LGG using SVM.

The following sections make up the order of this manuscript. Section 2 gives the information about the previous research works of brain tumour

segmentation and classification. Section 3 explains the proposed method. Section 4 presents a detail of the experimental setup of this manuscript. Section 5 compare the results with state-of-the-art methods and discussed. Section 6 conclude the manuscript.

2. RELATED WORKS

The technique of locating and delineating tumour locations within MRI brain scans is known as brain tumour segmentation. In the past decade lot of automatic technique was developed, Alagarsamy et al. (2019) developed new technique to find the tumour region from MRI images. This technique used the artificial bee colony based fuzzy-c means clustering technique. It is implemented on BraTS2015 dataset and got the DSC of 96.2% [8]. A lightweight hierarchical convolution network was created by Wang et al. (2021) to segment brain tumours. This approach produces good performance utilising the hierarchical convolution with residual connections and multi-scale strategy methods. It has less computation and used the BraTS2018 and 2020 dataset brain tumour images [9].

A new tumour classification and segmentation method was proposed by Ramprasad et al. (2022) In the feature extraction, it employed the gray-level cooccurrence matrix with redundant discrete wavelet transform, and for image segmentation, it used hybrid fuzzy c-means integrated k-means clustering technique. It achieved 99.46% classification accuracy and 99.21% segmentation accuracy. This method's primary flaw is that it used images from both CT and MRI scans [10]. Using Deep-Net, Shoushtari et al. (2022) devised an automated approach for segmenting brain tumours. The Atrous spatial pyramid pooling module was also utilised for the extraction of multiscale contextual information. It is implemented in the BraTS 2020 dataset images and got 97.5% segmentation accuracy. the drawback of this method is it used only the pre-trained Resnet18 weights [11].

Iqbal et al. (2022) developed U-Net based deep learning segmentation method for brain tumour. In this method BraTS 2018 all four MRI-multimodal high-grade and low-grade images are used. In the preprocessing step all NIFTI images are convert into 3D Numpy array. This method got the DSC score of 97% and 99% for HGG and LGG respectively [12]. The disentanglement learning framework technique is proposed by Liu et al. (2023) This method used the privileged semi-paired MRI images of BraTS2018 and 2020. It got the good quantitative and qualitative results. The drawback of this method is it did not focus the class imbalance of the BraTS dataset images [13].

A hierarchical multi-scale brain tumour segmentation network was created by Zhang et al. (2023) This approach made use of the multi-resolution feature fusion module and the lightweight conditional channel weighting block. It is implemented in BraTS2020 dataset images. It got the DSC for ET - 0.781, WT - 0.901, TC - 0.823. The drawback of this method is it used the two additional datasets were for comparative experiments [14]. Multi-input Unet model for brain tumor segmentation is proposed by Fang et al. (2023) It used the ablation experiment technique and implemented in the BraTS dataset. This method got the accuracy of 0.92 for whole tumour and 0.90 for tumour lesion. The drawback of this method is it did not find the enhanced tumour areas [15].

Mahum et al. (2023) developed the new technique in the combination of feature fusion and segmentation. It is implemented two datasets: Harvard and Figshare. This method used the ResNet-V2 and oriented gradient histogram for feature extraction and multilevel kapur's threshold technique with mayfly optimization algorithm for segmentation. This technique is not implemented in the BraTS dataset images [16]. Ozkaya et al. (2023) proposed classification and segmentation technique for brain tumours. This method used the CNN for tumour classification and Histogram algorithm for tumour segmentation. It is implemented on BraTS2020 dataset images. The drawback of this method is it achieves only 70.58% DSC segmentation accuracy [17].

The 3D based U-net model was proposed by Gore (2023). This method used both 2D type and 3D type MRI images for segmentation with labelled indications. The drawback of this technique is it use the merged dataset and also it compares the results only with the SegNet [18]. Maani et al. (2024) developed tumour segmentation method based on CNN for diverse populations. This method used the two convolutions depth-wise and point-wise with MedNeXt architecture. There are two sections to the dataset: training and validation with all model size of small, base, medium and large. It achieves DSC score of 85.54% on validation set images [19].

Context transformer architecture with 3D U-Net based tumour segmentation method was proposed by Nguyen et al. (2024) This technique is implemented on BraTS2019 dataset images. It achieves the DSC score of 89%, 81.5% and 82% for WT, TC and ET respectively. The drawback of this method is low training images [20]. A new federated automatic brain tumour segmentation method was developed by Giri et al. (2024) This method combines the U-Net with ResNet, and it is implemented on BraTS 3D type MRI images. It got the DSC score of 79%. The drawback of the method is it used the MRI

images for segmentation without any proper training [21]. Sourabh et al. (2024) developed the 3D U-Net based brain tumour segmentation method. It is implemented on the BraTS2020 dataset. This method used the emphasizes for data pre-processing and model optimization for clinical integration. It uses only low features for segmentation [22].

From the above all related works this research finds the following research gap. The major drawback is it extracts low features for segmentation so it got low accuracy. To overcome this problem this manuscript, suggested a M-VGG19 with SVM for segmentation and tumour grade classification. This method finds the LBP features and combined with M-VGG19 for best segmentation results with high accuracy, and it gives high training for improves the classification accuracy.

3. PROPOSED METHOD

This section gives full details about the proposed method of this manuscript. This method has three stages: pre-processing, segmentation and post-processing. In the BraTS2020 dataset the images of T2W, T1C and FLAIR has sub tumour information, the proposed method extracts the information and plotted onto the T1W images. The clear and detailed workflow architecture is shown in Figure 3.

3.1 Pre-processing

Generally, the pre-processing method is used to reduce the computation complexity. This manuscript has four steps of pre-processing techniques. DICOM to NIFTI, Skull removal, Noise removal and resize. This manuscript used two types of datasets: BraTS2020 and MMHRC. The BraTS dataset images are already in the NIFTI format and also without any skull and noises so, it did not need the first three steps of pre-processing but, MMHRC dataset images must need the first three steps. The last step of resize is need for both dataset images.

3.1.1 DICOM to NIFTI

Most of the medical images are in the DICOM format. If we want to process those images it must convert into NIFTI format, it is specifically designed for neuroimaging data. The RadiAnt DICOM viewer tool converts all the MMHRC – DICOM format images into NIFTI format, it is an open-source tool [23].

3.1.2 Skull removal

The human brain is protected by the dense bone it is called by the name skull. In the segmentation process the skull is an unwanted

portion because it makes artifacts and noise. It also makes difficult to find the accurate tumour boundaries. The BET open-source tool used all the converted NIFTI images for skull removal. This tool used the thresholding technique to remove the skull portion [24]. The skull removal result is shown in Figure 4.

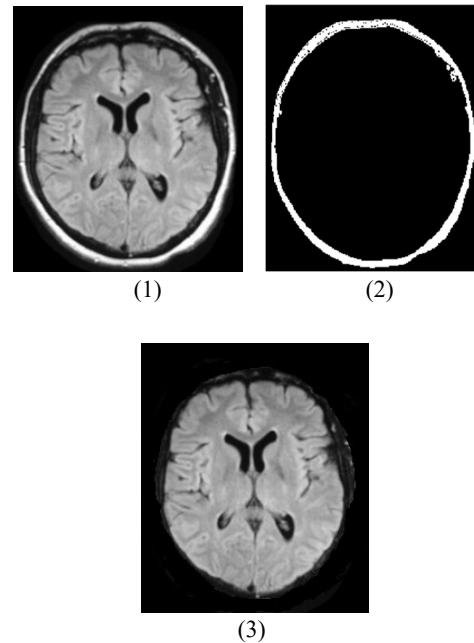


Figure 4: Skull removal using BET
(1) Original image with skull (2) Skull portion (outlier)
(3) Brain portion

3.1.3 Noise removal

Generally, the MRI machine produces the images with Rician noise, Gaussian Noise and Rayleigh noise. Gaussian filter helps to remove the noises from MR images. It utilises 3×3 convolutional masks, and the weighted average of neighbouring pixels is used to calculate the value of each pixel [25]. It computed as follow-

$$G_{\sigma, \mu}(a, b) = \frac{1}{2\pi\sigma^2} e^{-\frac{x^2+y^2}{2\sigma^2}} \quad (1)$$

Here, σ denotes standard deviation of the filter mask, μ indicates mean of the filter mask, horizontal axis distance from the origin is represented by x , while the vertical axis distance from the origin is represented by y .

3.1.4 Resize

All BraTS2020 dataset images are in 3D format in the same size of $240 \times 240 \times 155$. The MMHRC images are also in 3D format but not in the above size, each image is in the different sizes. So, the resize technique is implemented here to follow the same size for all MRI images. The resizing process is done by MATLAB for both dataset images. This process is paving the way for fast and accurate segmentation. All the BRATS and MMHRC new resize images are in the dimension's height, breadth and depth $128 \times 128 \times 128$ respectively. One sample resize of MMHRC and BraTS 2020 image is shown in Figure 5.

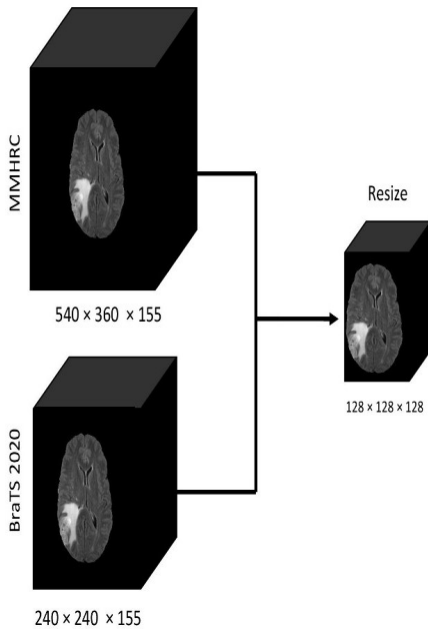


Figure 5: Resize image

3.2 Segmentation

This phase gives details about the segmentation process of a proposed method. It used the LBP features and M-VGG19 for brain tumour segmentation and implemented on both BraTS2020 and MMHRC dataset images. The LBP extracted features are given as an input to M-VGG19 for accurate segmentation.

3.2.1 Local binary pattern (LBP):

The proposed method uses the Local binary pattern (LBP) feature extractor. It is a straightforward yet powerful feature descriptor that is frequently applied to computer vision applications, such as the segmentation of brain tumours. This technique is particularly well-suited for texture analysis, which is crucial for

distinguishing tumour regions from healthy brain tissue. The all BRATS and MMHRC images are in the size of $128 \times 128 \times 128$ and the LBP use the 3×3 matrix to find the features from the images. The 3×3 matrix has 9 values, first it takes the centre value and compare with all other neighbour values [26]. It computed as follow-

$$LBP = \sum_{n=0}^7 (in - ic) 2^n$$

$$S(z) = \{ 1, z \geq 0 \text{ and } 0, z < 0 \} \quad (2)$$

Here, in – neighbour pixel value, ic – centre pixel value. If the final value of z is greater than or equal to zero the LBP value is one (1) and z is less than zero the LBP value is zero (0). In the following 3×3 matrix is computed using the EQ (2), here the centre pixel is 4 and the neighbour pixels are 5, 9, 1, 6, 3, 2, 7 and 4. It gives the binary values 1, 1, 0, 1, 0, 0, 1, 1 and produce the decimal value 211. One sample 3×3 matrix computation is shown in Figure 6.

3.2.2 Modified VGG19 (M-VGG19):

This manuscript uses the Modified VGG19 for segmentation. It is a convolutional neural network (CNN) architecture that is 19 layers deep. It was developed by the Visual Geometry Group (VGG) at the University of Oxford. It used for semantic segmentation and instance segmentation. The above extracted LBP features are given as an input to this M-VGG19. Generally, VGG19 has 47 layers with 46 connections but the proposed method modified the VGG19 by 52 layers with 51 connections. It removes some layers and added some new layers for more accurate segmentation.

Input layer - The 3D type input layer is used in the size of $128 \times 128 \times 128$.

Convolution layer – it is a basic component of CNN used to extract features from the input images, here LBP features are added. It computed as follow-

$$C_{out} = \left\lceil \frac{C_{in} + 2P - K}{S} \right\rceil + 1 \quad (3)$$

Here, C_{in} - input features, C_{out} - output features, P - padding size, K - kernel size, S - stride size.

Rectified Linear unit (ReLU) layer – It is a non-linear function to activate the network. It computed as follow-

$$ReLU = \max(0, x) \quad (4)$$

Here, x is an input value.

Clipped ReLU – it is a variant of the traditional ReLU activation function that introduces a threshold to limit the maximum output value. This helps to prevent the activations from becoming excessively large, which can lead to numerical instability and slow convergence during training. It computed as follow-

$$Clipped\ ReLU = \min(\max(0, x), clip\ value) \quad (5)$$

Pooling layer – it is a crucial component of CNN that downsamples the feature maps created by the previous convolutional layer. It retains the most significant information while decreasing the feature maps spatial size. There are two varieties of the pooling layer: average pooling and max pooling. The M-VGG19 utilize the max pooling layer technique. It computed as follow-

$$\max\ pool(x, y) = \max(a, b) \quad (Input(x.s + a, y.s + b)) \quad (6)$$

Here, input- input feature map, s – stride, a, b – dimensions of the pooling layer, x, y – coordinates of the output feature map.

Fully Connected Layer – generally it is the final layer before the output layer. It serves to integrate the high-level information extracted by the convolutional and pooling layers into a single vector representation.

Dropout Layer – it helps to stop overfitting by randomly dropping units (neurons) in the training.

Softmax Layer – it is a regularly utilised activation function in the last layer for classification tasks. It creates a probability distribution across the possible classes using the output of the previous layer.

Classification layer - it is typically the final layer that produces the predicted class or category. The

modified VGG19 architecture is shown in Figure 7.

Here, this M-VGG19 uses all the BraTS2020 and MMHRC multimodal T2W, T1C and FLAIR images for segmentation. During the segmentation this method has 221 training, 74 validation of BraTS images and 95 (74-BraTS2020 + 21-MMHRC) testing images. The FLAIR type MRI image has the clear visibility of whole tumour portions, T2W type MRI image has the clear visibility of enhanced tumour portions and finally, T1C type MRI image has the clear visibility of tumour core portions. The M-VGG19 combined all the LBP features and convolution features to accurately segment the tumour cells from the normal cells. Next, the segmented portions are compared with ground truth images to find the accuracy of the proposed method but, this is only possible for BraTS not for MMHRC images because MMHRC dataset did not has ground truth images. The modified VGG19 layers and parameters are shown in Table 1.

Loss function:

The dice loss function, which is frequently used in image segmentation applications, was employed in the proposed method. It is particularly effective when dealing with imbalanced datasets like BraTS. The major goal of this function to minimize the overlap between predicted and ground truth regions. It Handles imbalanced datasets well and minimizes the false positives and false negatives. It computed as follow-

$$Dice\ Loss = 1 - Dice\ Coefficient \quad (7)$$

Here, dice loss of 0 means perfect prediction, while a dice loss of 1 indicates no overlap.

3.3 Post-processing

This phase gives details about the post-processing of a proposed method. It has two steps: find the tumour volume and tumour Grade classification.

3.3.1 Find the tumour volume:

The previous segmentation phase WT, TC and ET tumour portions are mapped onto the T1W images of both datasets. Those T1W images and, BraTS2020 ground truth images are given as an input for the RadiAnt DICOM to find the tumour volume. The volume is predicted then the deviation is calculated between the segmented and ground truth images to know the accuracy. The deviation calculation process is only suitable for

BraTS2020 dataset because MMHRC dataset did not have ground truth images. The volume is calculating from the pixel height (pH) and pixel width (pW) of the tumour portions, those values are multiplied by slice thickness (st). The tumour volume find is shown in Figure 8. The tumour volume is computed as follow-

$$Tumour\ volume\ (mm^3) = pH \times pW \times st \quad (8)$$

The Brats2020 dataset images has st – 1(millimetre) mm³ and MMHRC images has st – 5mm³. All the tumour volumes are calculated in mm³ size format and convert into centimetre (cm³) format. It computed as follow-

$$Tumour\ volume\ (cm^3) = volume\ (mm^3) * 1000 \quad (9)$$

3.3.2 Tumour Grade classification:

This step uses the SVM for tumour Grade classification, it is a supervised machine learning technique. It is effective for high-dimensional data and complex decision boundaries [27]. It has two types of classifications: binary class and multi-class. The proposed method used the binary SVM (B-SVM) classification technique because the tumour is classified into two types of grades: HGG and LGG. The previous step BraTS2020 – 74 testing images are used for training (training + validation) and MMHRC – 21 images are used for testing.

Overall, 95 (74+21) images tumour volumes are predicted from the EQ (13) and EQ (14). The tumour grades are denoted by the following class labels: 0 (HGG), 1 (LGG). The HGG tumour volume range is above 100 cm³ and, LGG tumour volume is below 100 cm³. The classification process is done by using the MATLAB. The 2 × 2 general format confusion matrix is shown in Figure 9.

		Predicted Class	
		0	1
True Class	0	True Positive (TP)	False Negative (FN)
	1	False Positive (FP)	True Negative (TN)

Figure 9: The 2 × 2 general format confusion matrix

This technique fixes as Epoch - 100, Iteration - 30 and learning rate - 0.01. When each

iteration was completed, the images are shuffled and new features are learned by the machine. The overall elapsed time of the proposed method is 24 minutes 27 second. The accuracy percentage is denoted by blue color, loss percentage is denoted by red color and validation is denoted by black dots. The proposed method got the low loss and high validation accuracy of 99.13%. The proposed method B-SVM classification is shown in Figure 10.

4. EXPERIMENTAL SETUP

This section explained the experimental setup of this manuscript. Section 4.1 explains the dataset collection details for training and testing for the method. Section 4.2 explains the software and hardware tools used for this method. Section 4.3 explains the metrics to calculate the proposed method performance.

4.1 Dataset

This manuscript uses two types of datasets: BraTS2020 and real time brain tumour patient MRI images collect from the local hospital for brain tumour segmentation.

4.1.1 BraTS2020

The BraTS2020 dataset is an online open dataset is also used in the RSNA-ASNR-MICCAI challenge. It has 369 glioma type brain tumour patient images in two formats: HGG (259 images) and LGG (110 images). The all T1W, T2W, T1C and FLAIR multimodal images are in the size of 240 × 240 × 155 in 3D type with 1mm³ slice format. The dataset is fragmented into three sections: Training, Validation and Testing. The training has 221 images, validation has 74 images and testing has 74 images with Ground truth data [28].

4.1.2 Real time images

This method collects 21 real time brain tumour patient MRI images from the Meenakshi mission hospital and research centre (MMHRC), Madurai [29]. Each MRI images are in different size format with three different planes: axial, sagittal and coronal. The axial plane shows horizontal view, sagittal shows side-to-side view and coronal shows front-to-back view of the human body. These also has 5mm³ slice format. In the BraTS dataset, all images are in the coronal plane format so, this method commonly follows the coronal view format for both datasets. Real time MRI images different types of planes are shown in Figure 11.

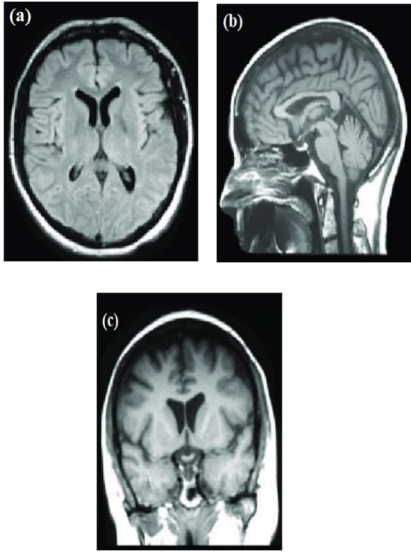


Figure 11: MMHRC dataset with three planes
(a) axial (b) sagittal (c) coronal

4.2 Tools

This work uses the RadiAnt DICOM viewer tool to convert the Digital imaging & communications in medicine (DICOM) format images into Neuroimaging informatics technology initiative (NIFTI) format images and also, it is used to find the tumour volume. The Brain extraction tool (BET) is used to remove the skull portion from the MRI images. The segmentation process is done by MATLAB R2021a (academic version) with the processor of 11th Gen intel®i7-11700K@5GHz and 16GB RAM. This proposed method also used the GPU parallel architecture. The Nvidia Quadro K5000 GPU provided by Nvidia Corporation in the configuration of 4GB of GDDR5, a memory bandwidth of 173 GB/s, 1.4-GHz processor, 1536 streaming cores is configured and eight multiprocessors are configured [2].

4.3 Metrics

This manuscript uses Sensitivity (SEN), Specificity (SPC) and Accuracy (ACC) metrics are used for classification. DSC and Hausdorff distance - 95th percentile (HD95) metrics are used for segmentation.

SEN - It is also called by the name Recall. It is a proportion of true tumour pixels that are correctly classified as tumour pixels. It computed as follow-

$$Sensitivity = \frac{TP}{TP+FN} \quad (10)$$

SPC - The proportion of true non-tumour pixels that are correctly classified as non-tumour pixels. It computed as follow-

$$Specificity = \frac{TN}{TN+FP} \quad (11)$$

ACC - The overall proportion of correctly classified pixels. It computed as follow-

$$Accuracy = \frac{TP+TN}{TP+TN+FP+F} \quad (12)$$

DSC - It is one of the similarity metrics used to quantify the overlap between two collections of data. It is computed using the ground truth mask and the predicted mask [30]. It computed as follow-

$$DSC = \frac{2TP}{2TP+FP+FN} \quad (13)$$

Here, TP - True positive, TN - True negative, FP - False positive and FN - False negative.

TP - Correctly predicted as tumour (actual tumour, predicted tumour).

TN - Correctly predicted as not tumour (actual not tumour, predicted not tumour).

FP - Incorrectly predicted as tumour (actual not tumour, predicted tumour).

FN - Incorrectly predicted as not tumour (actual tumour, predicted not tumour).

HD95 - It is a specific statistic used to calculate a segmentation model's accuracy. It calculates the distance between the ground truth tumour region and the projected tumour region [31]. It computed as follow-

$$HD95 = \min\{d: |\{x \in A : d(x, B) \leq d\}| \geq 0.95 * |A|\} \quad (14)$$

Here, A - predicted tumour region, B - ground truth tumour region, $d(x, B)$ - Euclidean distance between x and nearest point in B , $|\{x \in A : d(x, B) \leq d\}|$ - number of points in A that are within distance d of a point in B and $|A|$ - total number of points in A .

Speedup folds (\times) - It used to find the proposed method processing efficiency. It computed as follow-

$$\text{Speedup folds } (x) = \frac{\text{Processing time of CPU}}{\text{Processing time of GPU}} \quad (15)$$

5. RESULTS AND DISCUSSIONS

This section gives details about the proposed method M-VGG19 segmentation results, then predicted tumour volume results by RadiAnt DICOM and finally, tumour grade classification results by B-SVM for MMHRC dataset images using BraTS2020.

5.1 Segmentation results

The segmentation results are divided into two sections quantitative and qualitative for both Brats2020 and MMHRC dataset images.

5.1.1 Quantitative results of BraTS2020 and MMHRC

From the BraTS2020 dataset 221 training images, 74 validation images and 74 testing images are used for segmentation. The LBP and M-VGG19 features were gathered from every image and stored in the neural network. When new features appear, the neural network is updated to incorporate the newly discovered features. During the training time the proposed method got DSC of 0.9121, 0.8823, 0.8678 and HD95 of 4.56, 13.56, 13.77 and in the validation, it got DSC of 0.9285, 0.8856, 0.8602 and HD95 of 3.85, 12.95, 13.21. Finally, in the testing time it got DSC of 0.9415, 0.8898, 0.8862 and HD95 of 5.65, 11.11, 11.88 and for WT, TC and ET respectively. The training, validation and testing details are given in Table 2.

From the MMHRC dataset 13 training images, 4 validation images and 4 testing images are used for segmentation. During the training time the proposed method got DSC of 0.8625, 0.8474, 0.8012 and HD95 of 16.23, 13.56, 14.77 and in the validation, it got DSC of 0.8695, 0.8588, 0.8095 and HD95 of 16.12, 14.26, 15.02. Finally, in the testing time it got DSC of 0.8702, 0.8433, 0.8826 and HD95 of 16.11, 13.91, 15.77 and for WT, TC and ET respectively. The training, validation and testing details are given in Table 3.

The proposed method M-VGG19 results are compared with the eight state-of-the-art methods. Our proposed method outperforms all other previous methods in terms of all metrics. The M-VGG19 plays a major role for best results, because it observes all features from the images and do the segmentation very clearly. The dice loss function also easily managed the class imbalance problem So, the proposed method efficiency is increased to accurate segmentation. The segmentation result was found from the EQ (4) and

EQ (5). The BraTS2020 dataset proposed method M-VGG19 result comparison with state-of-the-art method is given in the Table 4.

Table.4 shows the comparison of the proposed method with eight state-of-the-art methods for tumour segmentation. These methods used different segmentation techniques to segment the tumour regions. Wang et al. developed modality pairing learning method. It got 89% of DSC and 6.24 of HD95 for whole tumour, due to the paring loss in the MRI images [32]. Agravat et al. used 3D fully convolutional neural network. It got only 87% of DSC and 8.30 HD95 for whole tumour. The major reason for this results this method used the parametric ReLU function and also additional inputs are needed between the layers in dense connections [33].

Zhao et al. used the multi-view point wise U-Net method. It got 83% of DSC and 10.36 HD95 for whole tumour, due to this method used the three views of MRI images: axial, sagittal, coronal and also the 3D images are replaced by 2D Multiview So, some patches are missing. [34]. Next, compare with Ali et al. this method used the ensemble 2D and 3D U-Net modal and got 87% of DSC and 8.09 of HD95 for whole tumour. The major reason for this results this method transform the 2D information to 3D with the help of dimension transform but it used only in the early layers [35]. Russo et al. developed deep convolution neural network with spherical coordinates transformation method for segmentation and got 86% of DSC and 6.73 of HD95. The reason for this results this method used the adjusted input shape and loss function so, every time the input value is adjusted [36].

Next, compare with Sundaresan et al. this method used triplanar ensemble network for segmentation. It got 89% of DSC and 6.30 of HD95 for whole tumour, due to this method reduced the depth of the U-Net in each plane [37]. Henry et al. developed self-ensembled with deeply supervised 3D U-Net method. It got 88% of DSC and 6.66 of HD95 for whole tumour. The reason for this results this method used two independent models were used and then their features are mapped in the images and when merged images the features are mismatched [38]. Next, compare with Anand et al. developed 3D convolution neural network with hard mining. It got 85% of DSC and 8.07 of HD95 for whole tumour, due to low pre-processing and low patch extraction [39].

Finally, the proposed method gives best results for segmentation and the usage of Nvidia GPU is minimize the computation time.

The graphical representation of the proposed technique is exposed in Figure.12 and 13.

The Figures 12 and 13, clearly explains the proposed method got best result compare with other methods. In the Figure 12 left hand side denote the accuracy, the DSC accuracy is fixed 0 as minimum and 1 as maximum. In the Figure 13 left hand side denote the distance. The HD95 distance is fixed 0 as starting range and ending range is depends upon the image. In the both Figures WT is denoted by blue color, TC is denoted by grey color and, ET is denoted by orange color. Generally, the CPU takes 5 seconds per image and totally it takes 2 hours 4 seconds for segmentation 295 images (training + validation) but the parallel computing toolbox in MATLAB with GPU takes 2 seconds per image and totally it takes only 49 minutes for the above same segmentation. So, the proposed method was rush up in to $3\times$ approximately from the EQ (15).

5.1.2 Qualitative results of BraTS2020 and MMHRC

In the following table the first column gives the details about the dataset. The second column mention about the image type. The third, fourth and fifth columns denote the segmented area of WT, TC and ET respectively. The sixth column denote the mapped sub-regions onto the T1W image. The seventh column denote the ground truth images and finally, the eighth column denote the full segmented areas from T1W image. In the FLAIR images WT portions are denoted by the yellow color. In the T2W images TC portions are denoted by the red color and in the T1C images ET portions are denoted by the green color. The proposed method qualitative segmentation outcomes are given in Table 5.

5.2 Predicted Tumour volume

The 74 - BraTS2020 training images and the 21 - MMHRC dataset testing images are used in this part to forecast the tumour volume. The Radiant DICOM predict the complete tumour volume from both dataset images. The tumour volumes are predicted in 3D format and calculated by cm^3 metric using the EQ (13) and EQ (14). In the following table column one denotes the dataset name, column two mentioned the image type, column three mentioned the 3D tumour image, column four, five, six mentioned pH , pW , st values respectively. The seventh column mentioned the complete tumour volume in cm^3 . Some sample 3D tumour images and their predicted volumes are given in Table 6.

The predicted tumour volume is compared with ground truth image tumour volume to find the accuracy. Some sample tumour volume deviation is given in the following table. From the below table HGG and LGG type has the difference of 0.38 cm^3 and 0.59 cm^3 respectively. So, there is no major deviation occur in our proposed segmentation method M-VGG19. The tumour volume comparison results are given in Table 7.

5.3 Classification results

The previous step predicted tumour volumes of the Brats2020 – 74 images are used for training and MMHRC – 21 images are used for testing in B-SVM. The confusion matrix of the training and testing details are shown in Figure.14.

From the Figure.14 (i) the B-SVM correctly classified the 36 images are HGG and 35 images are LGG. 1 HGG images wrongly classified as LGG and 2 LGG images wrongly classified as HGG images. From the Figure.14 (ii) the B-SVM correctly classified the 9 images are HGG and 9 images are LGG. 2 HGG images wrongly classified as LGG and 1 LGG image is wrongly classified as HGG image. The classification results are found from the EQ (1) to EQ (3). The B-SVM tumour grade classification training and testing details are given in the Table 8.

From the EQ (13) and EQ (14) the proposed method finds the HGG and LGG tumour volume. The proposed method used fitsvm for binary classification [40]. The SVM fixed the standard boundary line value is 138.25 cm^3 than it starts the classification. If the tumour volume is below the boundary line value those tumours are labelled LGG tumour (1), next if the tumour volume is equal to the boundary value and high to the boundary value those tumours are labelled HGG tumour (0). In this figure HGG tumours are denoted by red color dots and LGG tumours are denoted by green color dots. The support vectors are denoted by the black circle. The SVM boundary line is denoted by violet continues line, upper margin is denoted by blue dotted line and lower margin is denoted by red dotted line. The SVM boundary-based classification is shown in Figure15.

From the Table.8 the B-SVM training got the sensitivity, specificity, accuracy of 97.29%, 94.59%, 95.94% respectively and, the testing got sensitivity, specificity, accuracy of 81.81%, 90%, 85.71% respectively. Due to the low images of MMHRC and its high slice thickness is the major reason for the low accuracy in testing.

6. CONCLUSION

This manuscript proposed efficient automatic brain tumour segmentation method M-VGG19. This technique is implemented on BraTS2020 and MMHRC dataset images. The proposed method is split into three stages: pre-processing, segmentation and post-processing. This technique finds the tumour volume and also find the grade of the MMHRC images. Compare the result with state-of-the-art methods the proposed method got DSC of 0.9415, 0.8898, 0.8862 and HD95 of 5.65, 11.11, 11.88 for WT, TC and ET respectively. The usage of GPU will increase the processing time 3× faster. The tumour grade classification got the 85.71 accuracy for MMHRC images. In the future, the proposed method is implemented in other online and real time images with some other advanced pre-processing techniques to improves the accuracy.

Declarations

Ethics approval and consent to participate

Not Applicable.

Consent for publication

Authors approve to consent for publications

Availability of data and materials

Real time dataset was obtained from MMHRC, Madurai.

Conflict of interest

The authors declare that they have no conflicts of interest.

Funding

This work does not involve any funding.

Acknowledgement

The authors did not want to thank anyone.

Authors' contributions

Syedsafi contributed to conceptualization, methodology and content writing.

Kartheeban contributed to ideology, design and document corrections.

REFERENCES:

- [1]. Alagarsamy, S., Kamatchi, K., Selvaraj, K., Subramanian, A., Fernando, L. R., & Kirthikaa,

R. (2019, December). Identification of Brain Tumor using Deep Learning Neural Networks. In 2019 IEEE International Conference on Clean Energy and Energy Efficient Electronics Circuit for Sustainable Development (INCCES) (pp. 1-5). IEEE.

- [2]. Shajahan, S., Pathmanaban, S., & Tiruvenkadam, K. (2024). RIBM3DU-Net: Glioma tumour substructures segmentation in magnetic resonance images using residual-inception block with modified 3D U-Net architecture. *International Journal of Imaging Systems and Technology*, 34(2), e23056.
- [3]. Alagarsamy, S., Kamatchi, K., & Govindaraj, V. (2019). An Automated Hybrid Methodology Using Firefly Based Fuzzy Clustering for Demarcation of Tissue and Tumor Region in Magnetic Resonance Brain Images. In *Advances in Computerized Analysis in Clinical and Medical Imaging* (pp. 193-208). Chapman and Hall/CRC.
- [4]. Syedsafi, S., Sriramakrishnan, P., Kalaiselvi, T. (2023). MR Image Block-Based Brain Tumour Detection Using GLCM Texture Features and SVM. In: Reddy, A.B., Nagini, S., Balas, V.E., Raju, K.S. (eds) *Proceedings of Third International Conference on Advances in Computer Engineering and Communication Systems*. Lecture Notes in Networks and Systems, vol 612. Springer, Singapore.
- [5]. Alagarsamy, S., Kamatchi, K., & Govindaraj, V. (2019, June). A Novel Technique for identification of tumor region in MR Brain Image. In 2019 3rd International conference on Electronics, Communication and Aerospace Technology (ICECA) (pp. 1061-1066). IEEE.
- [6]. Syedsafi, S., Sriramakrishnan, P., & Kalaiselvi, T. (2023, June). An automated two-stage brain tumour diagnosis system using SVM and geodesic distance-based colour segmentation. In *International Conference on Power Engineering and Intelligent Systems (PEIS)* (pp. 179-191). Singapore: Springer Nature Singapore.
- [7]. Rinesh, S., Maheswari, K., Arthi, B., Sherubha, P., Vijay, A., Sridhar, S., ... & Waji, Y. A. (2022). Investigations on brain tumor classification using hybrid machine learning algorithms. *Journal of Healthcare Engineering*, 2022(1), 2761847.
- [8]. Alagarsamy, S., Kamatchi, K., & Govindaraj, V. (2019, December). A novel technique based on artificial bee colony for MR brain image segmentation. In 2019 IEEE International Conference on Clean Energy and Energy

- Efficient Electronics Circuit for Sustainable Development (INCCES) (pp. 1-6). IEEE.
- [9]. Wang, Y., Cao, Y., Li, J., Wu, H., Wang, S., Dong, X., & Yu, H. (2021). A lightweight hierarchical convolution network for brain tumor segmentation. *BMC bioinformatics*, 22(Suppl 5), 636.
- [10]. Ramprasad, M. V. S., Rahman, M. Z. U., & Bayleyegn, M. D. (2022). A deep probabilistic sensing and learning model for brain tumor classification with fusion-net and HFCMIK segmentation. *IEEE Open Journal of Engineering in Medicine and Biology*, 3, 178-188.
- [11]. Shoushtari, F. K., Sina, S., & Dehkordi, A. N. (2022). Automatic segmentation of glioblastoma multiform brain tumor in MRI images: Using Deeplabv3+ with pre-trained Resnet18 weights. *Physica Medica*, 100, 51-63.
- [12]. Iqbal, M. J., Iqbal, M. W., Anwar, M., Khan, M. M., Nazimi, A. J., & Ahmad, M. N. (2022). Brain tumor segmentation in multimodal MRI using U-Net layered structure. *Comput Mater Contin*, 74(3), 5267-5281.
- [13]. Liu, Z., Wei, J., Li, R., & Zhou, J. (2023). Learning multi-modal brain tumor segmentation from privileged semi-paired MRI images with curriculum disentanglement learning. *Computers in biology and medicine*, 159, 106927.
- [14]. Zhang, R., Jia, S., Adamu, M. J., Nie, W., Li, Q., & Wu, T. (2023). HMNet: Hierarchical multi-scale brain tumor segmentation network. *Journal of Clinical Medicine*, 12(2), 538.
- [15]. Fang, L., & Wang, X. (2023). Multi-input Unet model based on the integrated block and the aggregation connection for MRI brain tumor segmentation. *Biomedical Signal Processing and Control*, 79, 104027.
- [16]. Mahum, R., Sharaf, M., Hassan, H., Liang, L., & Huang, B. (2023). A Robust Brain Tumor Detector Using BiLSTM and Mayfly Optimization and Multi-Level Thresholding. *Biomedicines*, 11(6), 1715.
- [17]. Özkaya, Ç., & Sağiroğlu, Ş. (2023). Glioma grade classification using CNNs and segmentation with an adaptive approach using histogram features in brain MRIs. *IEEE Access*, 11, 52275-52287.
- [18]. Gore, S. (2023). Brain tumour segmentation and Analysis using BraTS Dataset with the help of Improvised 2D and 3D UNet model.
- [19]. Maani, F. A., Hashmi, A. U. R., Saeed, N., & Yaqub, M. (2024, May). On Enhancing Brain Tumor Segmentation across Diverse Populations with Convolutional Neural Networks. In 2024 IEEE International Symposium on Biomedical Imaging (ISBI) (pp. 1-4). IEEE.
- [20]. Nguyen, T. Q. T., Nguyen, H. N., Bui, T. H., Nguyen-Tat, T. B., & Ngo, V. M. (2024, August). Brain Tumor Segmentation in MRI Images with 3D U-Net and Contextual Transformer. In 2024 International Conference on Multimedia Analysis and Pattern Recognition (MAPR) (pp. 1-6). IEEE.
- [21]. Giri, A., Thapa, P., Banu, J. S., Poudyal, S., Rijal, B., & Karki, S. (2024). Harnessing ResUHybridNet with Federated Learning: A New Paradigm in Brain Tumour Segmentation. *Revue d'Intelligence Artificielle*, 38(3), 765.
- [22]. Sourabh, S., Valliappan, M., & Darapaneni, N. (2024). Deep Learning-Based Brain Image Segmentation for Automated Tumour Detection. *arXiv preprint arXiv:2404.05763*.
- [23]. <https://www.radiantviewer.com/> (Accessed on 14 November 2024).
- [24]. <https://mangoviewer.com/mango.html> (Accessed on 14 November 2024).
- [25]. Yang, J., Fan, J., Ai, D. et al. Brain MR image denoising for Rician noise using pre-smooth non-local means filter. *BioMed Eng OnLine* 14, 2 (2015).
- [26]. Abbasi, S., & Tajeripour, F. (2017). Detection of brain tumor in 3D MRI images using local binary patterns and histogram orientation gradient. *Neurocomputing*, 219, 526-535.
- [27]. RM, V., Elsoud, M. A., & Alkhambashi, M. (2018). Optimal feature level fusion based ANFIS classifier for brain MRI image classification.
- [28]. <https://www.med.upenn.edu/cbica/brats2020/#:~:text=BraTS%202020%20utilizes%20multi%2Dinstitutional,%20brain%20tumors%2C%20namely%20gliomas>. (Accessed on 16 November 2024).
- [29]. <https://mmhrc.in/> (Accessed on 16 November 2024).
- [30]. Elmezain, M., Mahmoud, A., Mosa, D. T., & Said, W. (2022). Brain tumor segmentation using deep capsule network and latent-dynamic conditional random fields. *Journal of Imaging*, 8(7), 190.
- [31]. Saueressig, C., Berkley, A., Munbodh, R., & Singh, R. (2021, September). A joint graph and image convolution network for automatic brain tumor segmentation. In *International MICCAI Brainlesion Workshop* (pp. 356-365). Cham: Springer International Publishing.

- [32]. Wang Y, Zhang Y, Hou F, et al. Modality-pairing learning for brain tumor segmentation. Brainlesion: Glioma, Multiple Sclerosis, Stroke and Traumatic Brain Injuries: 6th International Workshop, BrainLes 2020, Held in Conjunction with MICCAI 2020, October 4, 2020, Revised Selected Papers, Part I 6. Springer International Publishing; 2021:230-240.
- [33]. Agravat RR, Raval MS. 3D semantic segmentation of brain tumor for overall survival prediction. Brainlesion: Glioma, Multiple Sclerosis, Stroke and Traumatic Brain Injuries: 6th International Workshop, BrainLes 2020, Held in Conjunction with MICCAI 2020, October 4, 2020, Revised Selected Papers, Part II 6. Springer International Publishing; 2021:215-227.
- [34]. Zhao C, Zhao Z, Zeng Q, Feng Y. MVP U-Net: multi-view pointwise U-net for brain tumor segmentation. Brainlesion: Glioma, Multiple Sclerosis, Stroke and Traumatic Brain Injuries: 6th International Workshop, BrainLes 2020, Held in Conjunction with MICCAI 2020, October 4, 2020, Revised Selected Papers, Part II 6. Springer International Publishing; 2021:93-103.
- [35]. Ali MJ, Akram MT, Saleem H, Raza B, Shahid AR. Glioma segmentation using ensemble of 2D/3D U-Nets and survival prediction using multiple features fusion. Brainlesion: Glioma, Multiple Sclerosis, Stroke and Traumatic Brain Injuries: 6th International Workshop, BrainLes 2020, Held in Conjunction with MICCAI 2020, October 4, 2020, Revised Selected Papers, Part II 6. Springer International Publishing; 2021:189-199.
- [36]. Russo C, Liu S, Di Ieva A. Impact of spherical coordinates transformation pre-processing in deep convolution neural networks for brain tumor segmentation and survival prediction. Brainlesion: Glioma, Multiple Sclerosis, Stroke and Traumatic Brain Injuries: 6th International Workshop, BrainLes 2020, Held in Conjunction with MICCAI 2020, October 4, 2020, Revised Selected Papers, Part I 6. Springer International Publishing; 2021:295-306.
- [37]. Sundaresan V, Griffanti L, Jenkinson M. Brain tumour segmentation using a triplanar ensemble of U-Nets on MR images. Brainlesion: Glioma, Multiple Sclerosis, Stroke and Traumatic Brain Injuries: 6th International Workshop, BrainLes 2020, Held in Conjunction with MICCAI 2020, Lima, Peru, October 4, 2020, Revised Selected Papers, Part I. Springer International Publishing; 2021, March:340-353.
- [38]. Henry T, Carré A, Lerousseau M, et al. Brain tumor segmentation with self-ensembled, deeply-supervised 3D U-net neural networks: a BraTS 2020 challenge solution. Brainlesion: Glioma, Multiple Sclerosis, Stroke and Traumatic Brain Injuries: 6th International Workshop, BrainLes 2020, Held in Conjunction with MICCAI 2020, October 4, 2020, Revised Selected Papers, Part I 6. Springer International Publishing; 2021:327-339.
- [39]. Anand VK, Grampurohit S, Aurangabadkar P, et al. Brain tumor segmentation and survival prediction using automatic hard mining in 3D CNN architecture. Brainlesion: Glioma, Multiple Sclerosis, Stroke and Traumatic Brain Injuries: 6th International Workshop, BrainLes 2020, Held in Conjunction with MICCAI 2020, October 4, 2020, Revised Selected Papers, Part II 6. Springer International Publishing; 2021:310-319.
- [40]. <https://in.mathworks.com/help/stats/fitcsvm.html> (Accessed on 17 November 2024).

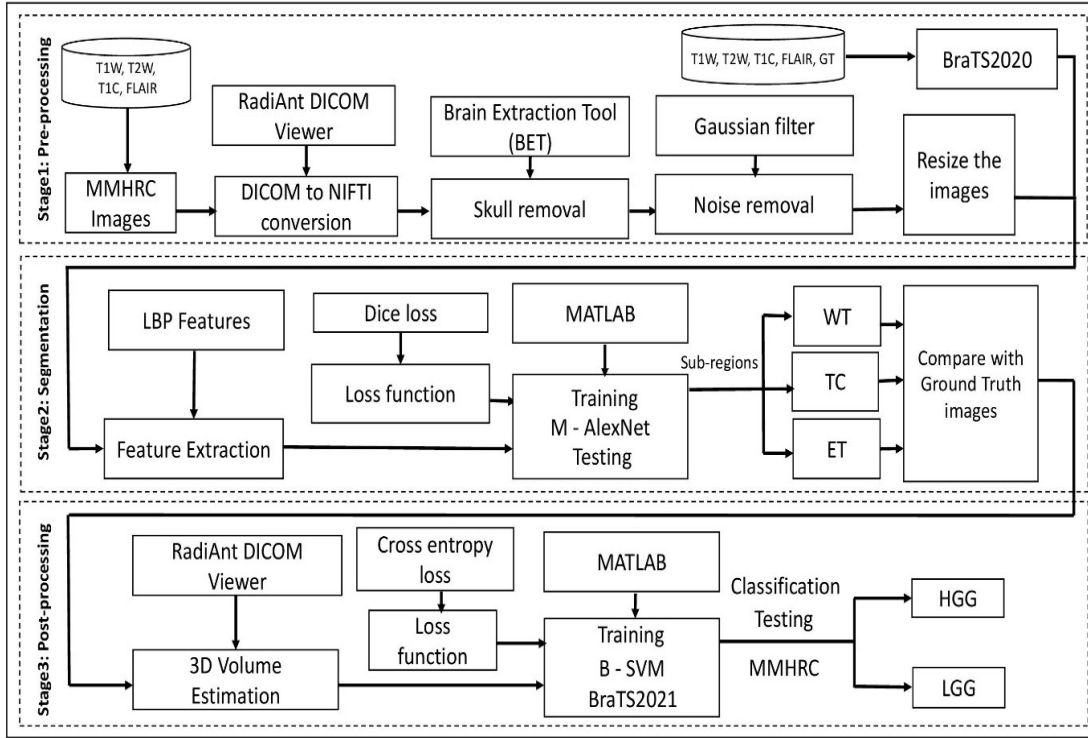


Figure 3: Proposed method detailed architecture

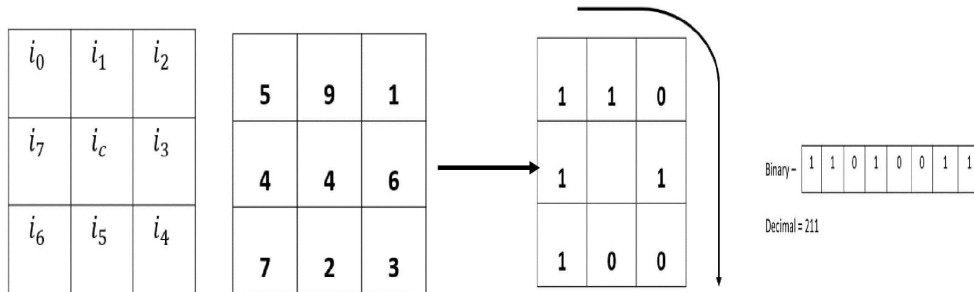


Figure 6: Sample 3×3 matrix to find the LBP feature.

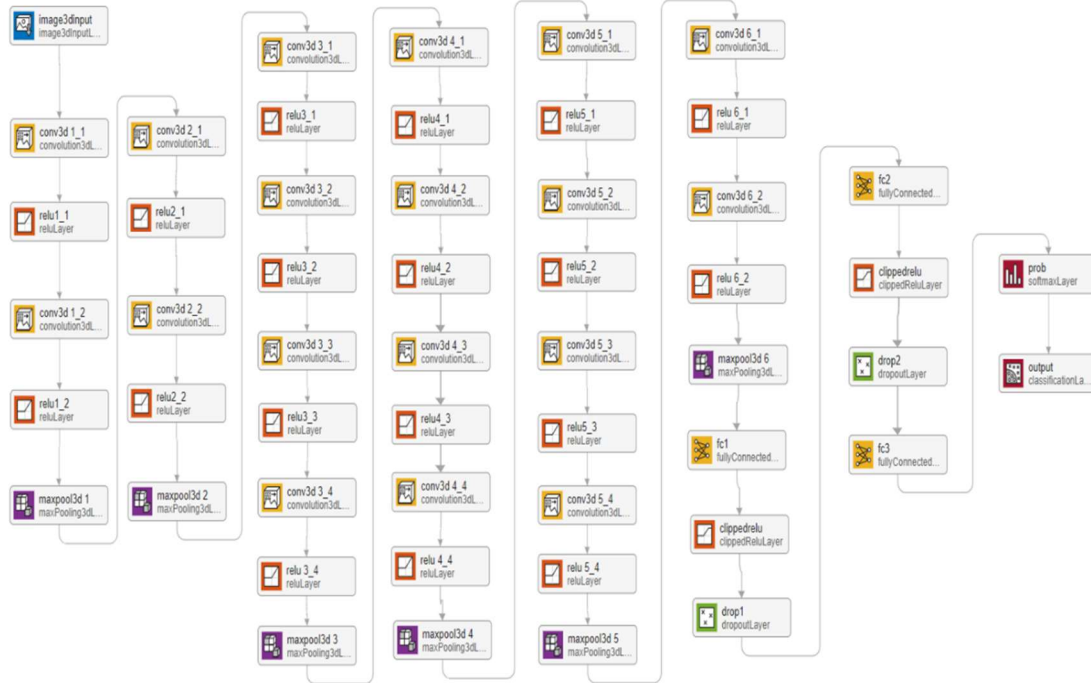


Figure 7: Modified VGG19 architecture.

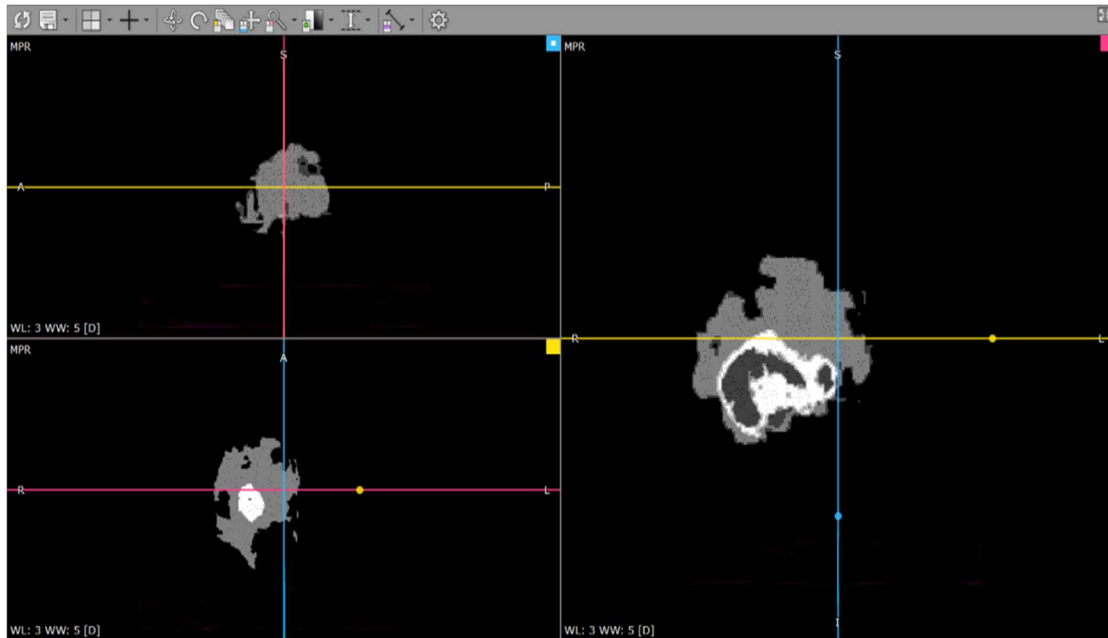


Figure 8: Tumour volume find

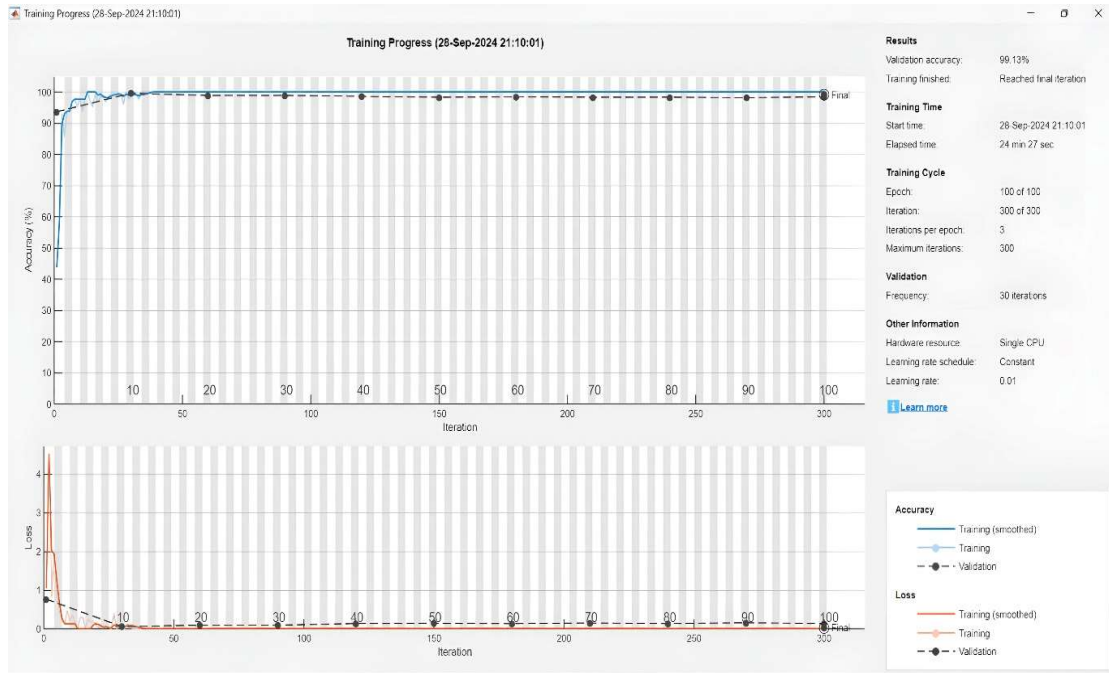


Figure 10: B-SVM classification

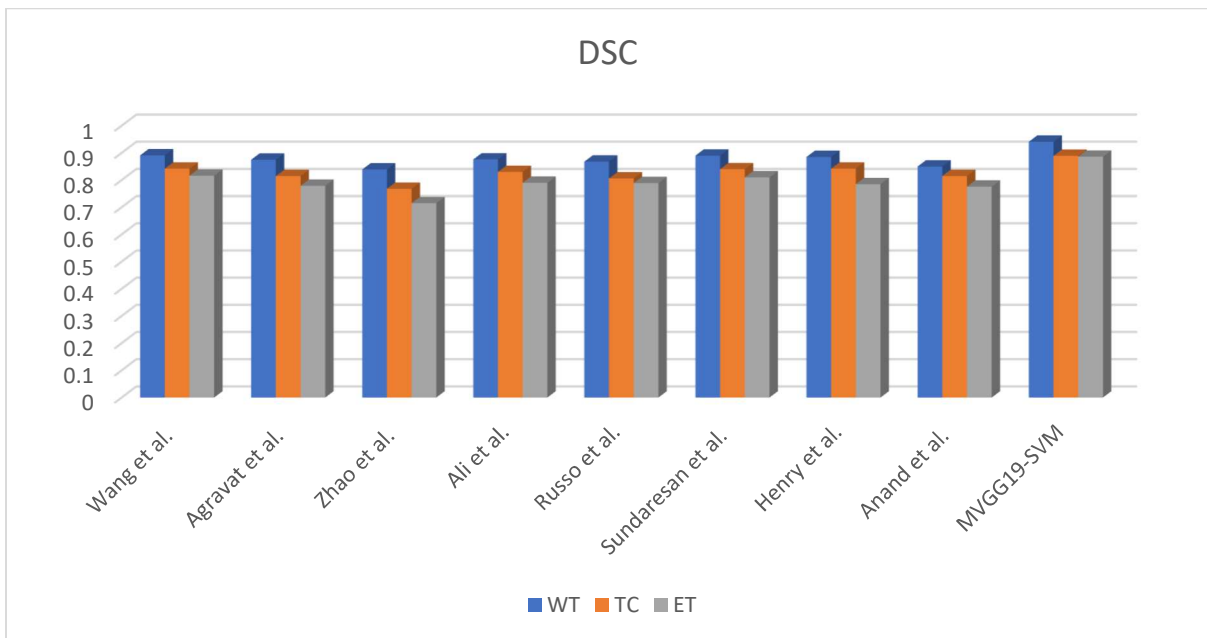


Figure 12: DSC comparison of Proposed method with state-of-art methods

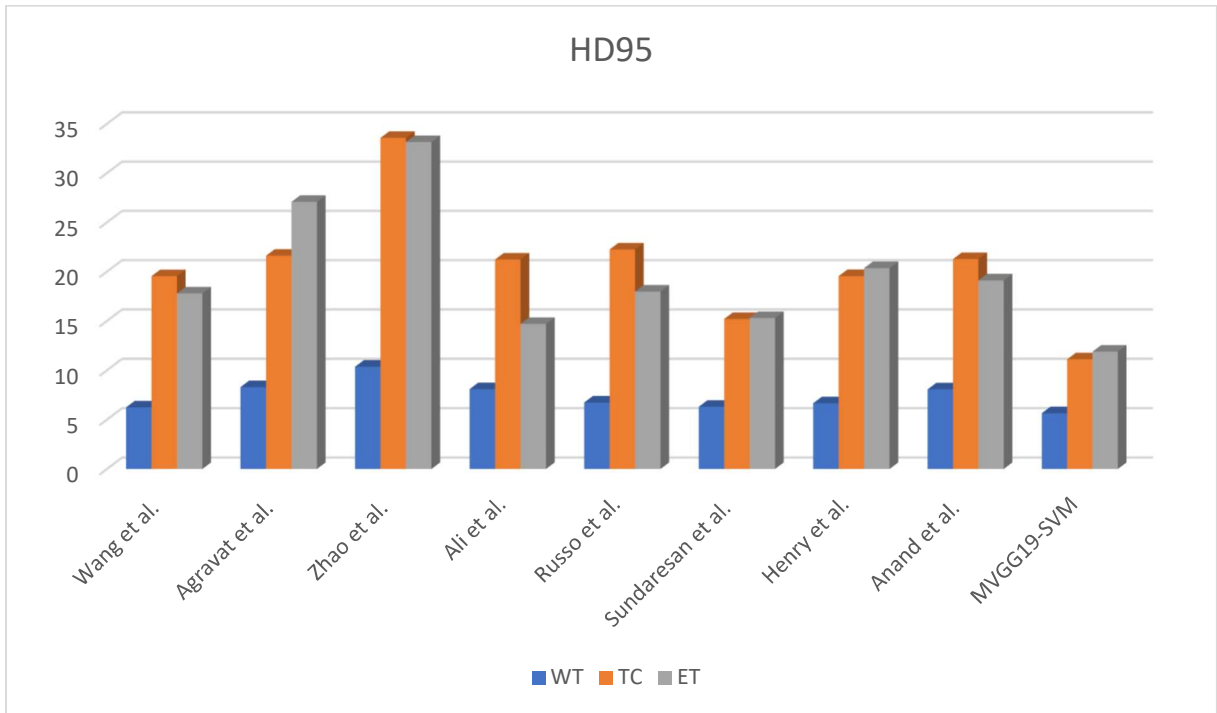


Figure 13: HD95 comparison of Proposed method with state-of-art methods

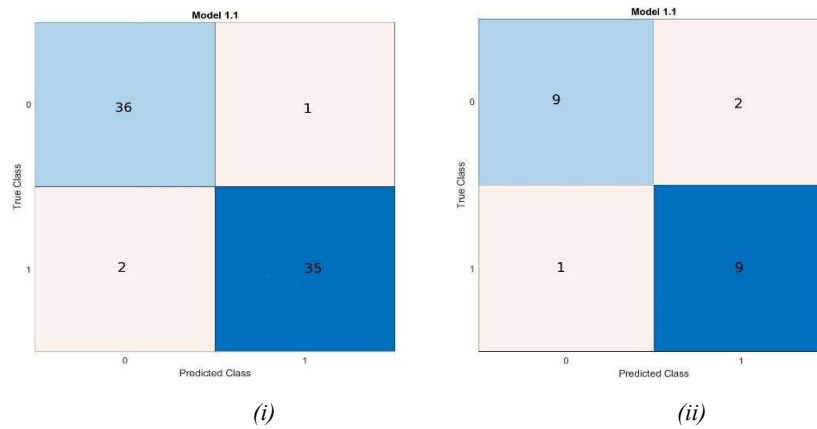


Figure 14: Confusion matrix (i) Training result (ii) Testing result

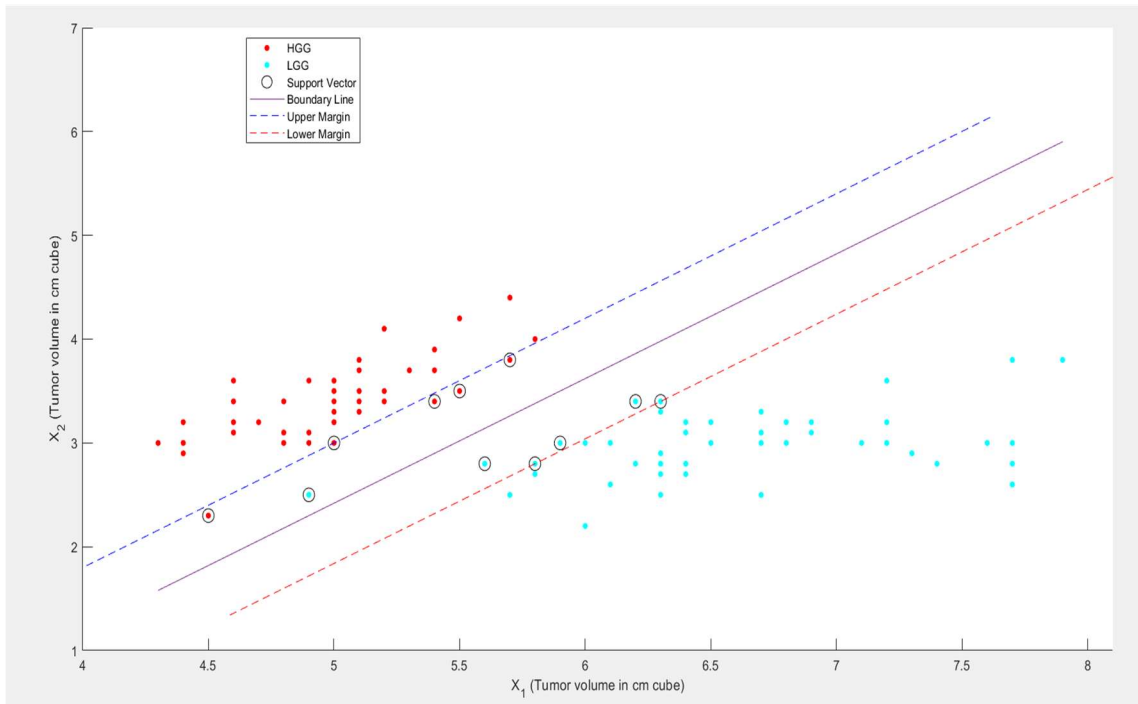


Figure 15: SVM classification

Table 1: Modified VGG19 layers and their parameters.

Level	Name of the Layer	Number of the layer	Parameters	Count of Layers
1	Image3Dinput	1	-	1
2	Convolution3D	1_1, 1_2 and 2_1, 2_2	Size of the filter - 3, 3, 3 Number of filters (No.F) - 32 Stride (S) - 1, 1, 1 Padding (P) - same	18
		3_1, 3_2, 3_3, 3_4	Size of the filter - 3, 3, 3 No.F - 64 S - 1, 1, 1 Padding - same	
		4_1, 4_2, 4_3, 4_4	Size of the filter - 3, 3, 3 No.F - 128 S - 1, 1, 1 P - same	
		5_1, 5_2, 5_3, 5_4	Size of the filter - 3, 3, 3 No.F - 512 S - 1, 1, 1 P - same	
		6_1, 6_2	Size of the filter - 3, 3, 3 No.F - 1024 S - 1, 1, 1 P - same	
3	ReLU	1_1, 1_2 2_1, 2_2 3_1, 3_2, 3_3, 3_4 4_1, 4_2, 4_3, 4_4 5_1, 5_2, 5_3, 5_4 6_1, 6_2	-	18
4	Clipped ReLU	-	-	2
5	Maxpooling3D	1, 2, 3, 4, 5, 6	Pool size - 5, 5, 5 S - 1, 1, 1 P - same	6
6	Fully connected	1, 2, 3	-	3
7	Dropout	1, 2	-	2
8	Softmax	-	-	1
9	Classification	-	-	1
Total Layers				52

Table 2: BraTS2020 Training, Validation and Testing results

Dataset	Type	No of Images	DSC			HD95		
			WT	TC	ET	WT	TC	ET
BraTS 2020	Training	221	0.9121	0.8823	0.8678	4.56	13.56	13.77
	Validation	74	0.9285	0.8856	0.8602	3.85	12.95	13.21
	Testing	74	0.9415	0.8898	0.8862	5.65	11.11	11.88

Table 3: MMHRC Training, Validation and Testing results

Dataset	Type	No of Images	DSC			HD95		
			WT	TC	ET	WT	TC	ET
MMHRC	Training	13	0.8625	0.8474	0.8012	16.23	13.56	14.77
	Validation	4	0.8695	0.8588	0.8095	16.12	14.26	15.02
	Testing	4	0.8702	0.8433	0.8826	16.11	13.91	15.77

Table 4: Comparison of the Proposed method with State-of-the-art methods for BraTS2020

S. No	Method	Dice			HD95		
		WT	TC	ET	WT	TC	ET
1.	Wang et al. [32]	0.891	0.842	0.816	6.240	19.540	17.790
2.	Agravat et al. [33]	0.875	0.815	0.779	8.302	21.611	27.078
3.	Zhao et al. [34]	0.839	0.768	0.715	10.362	33.577	33.147
4.	Ali et al. [35]	0.876	0.830	0.790	8.092	21.230	14.699
5.	Russo et al. [36]	0.868	0.806	0.789	6.734	22.247	17.974
6.	Sundaresan et al. [37]	0.890	0.840	0.810	6.300	15.200	15.300
7.	Henry et al. [38]	0.885	0.842	0.785	6.666	19.549	20.360
8.	Anand et al. [39]	0.850	0.815	0.776	8.070	21.276	19.110
9.	Proposed Method (MVG19-SVM)	0.941	0.889	0.886	5.650	11.112	11.889

Table 5: Qualitative results of BraTS2020 and MMHRC

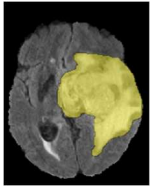
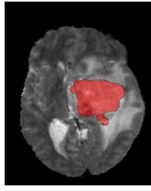
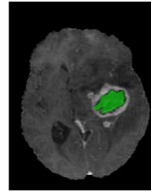
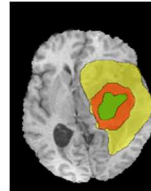
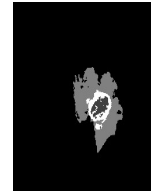

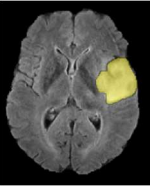
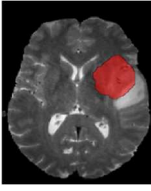
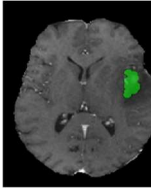
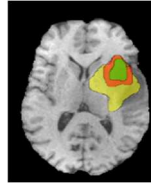
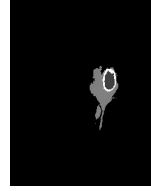

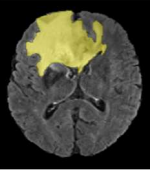
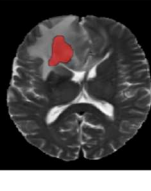
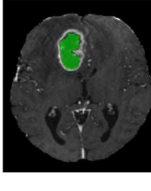
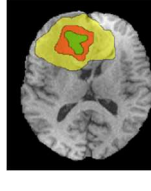


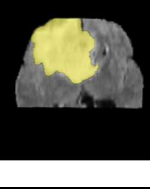
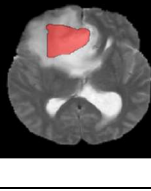
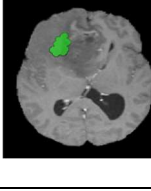
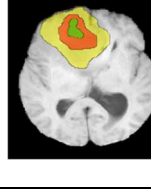
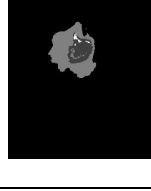
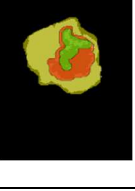
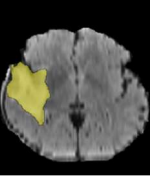
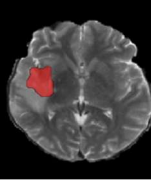
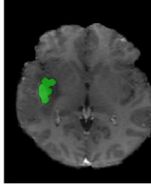
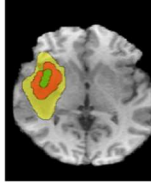


Dataset	Image Type	WT	TC	ET	Mapped onto T1W	GT	Segmented image
BraTS 2020	HGG						
	HGG						
	LGG						
	LGG						
MMHRC	-						

Table 6: Sample tumour 3D volume

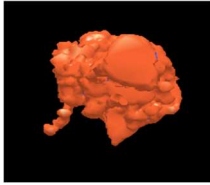
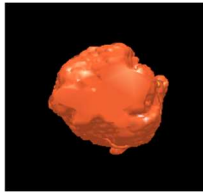
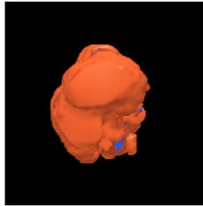
Dataset	Image type	3DTumour image	pH (mm ³)	pW (mm ³)	st (mm ³)	Tumour volume (cm ³)
BraTS 2020	HGG		0.485	0.321	1	156.49
	LGG		0.285	0.255	1	72.675
MMHRC	-		0.126	0.118	5	74.34

Table 7: Tumour volume comparison results

Dataset	Image type	Original Volume (cm ³)	Predicted volume (cm ³)	Deviation (cm ³)
BraTS 2020	HGG	156.87	156.49	0.38
	LGG	73.265	72.675	0.59

Table 8: B-SVM tumour grade classification

Type	No of images & Dataset	B-SVM Classification		
		Sensitivity (%)	Specificity (%)	Accuracy (%)
Training (Training + Validation)	74 (59 + 15) (BraTS 2020)	97.29	94.59	95.94
Testing	21 (MMHRC)	81.81	90	85.71